Chapter 4

The Weakly Interacting Electron Gas

4.1 The Electron Gas in Perturbation Theory

Consider an electron gas with a spin-independent instantaneous electron-electron interaction $U(x-y)$ described by the Hamiltonian H_1:

$$H_1 = \frac{1}{2}\int d^3x \int d^3y \; n(x)n(y)\; U(x-y) \tag{4.1}$$

where

$$n(x) = \sum_{\sigma=\uparrow,\downarrow} \psi^\dagger_\sigma(x)\psi_\sigma(x) \tag{4.2}$$

Then,

$$\int_{-\infty}^{+\infty} dt H_1(t) \;=\; \frac{1}{2}\int d^4x \int d^4y \; n(x)n(y)\; V(x-y) \tag{4.3}$$

where

$$V(x-y) \;=\; U(x-y)\delta(t-t') \tag{4.4}$$

In the perturbative evaluation of the Feynman electron propagator

$$G_F^{\nu\nu'}(x,x') = -i\langle G|T(\psi_\nu(x)\psi^\dagger_{\nu'}(x')|G\rangle \tag{4.5}$$

where $|G\rangle$ is the *exact* ground state of the interacting system, we will need to evaluate the expectation value the matrix element in the unperturbed ground

state:

$$ {}_0\langle G|T(\psi_\nu(x)\psi^\dagger_{\nu'}(x')\, e^{-\frac{i}{\hbar}\int_{-\infty}^{\infty} dt'' H_1(t'')})|G\rangle_0 \tag{4.6} $$

where $|G\rangle_0$ is the ground state of the unperturbed system. To lowest order in perturbation theory in H_1, we will need to compute the expectation value

$$ \frac{1}{2}\int d^4z \int d^4z' \sum_{\sigma\sigma'=\uparrow,\downarrow} V(z-z')\ {}_0\langle G|T(\psi_\nu(x)\psi^\dagger_{\nu'}(x')\psi^\dagger_\sigma(z)\psi_\sigma(z)\psi^\dagger_{\sigma'}(z')\psi_{\sigma'}(z))|G\rangle_0 \tag{4.7} $$

We will now use Wick's theorem to express this expectation value in terms of products of pair-wise contractions. We will denote a contraction by

$$ \overbrace{\psi_\nu(x)\psi^\dagger_{\nu'}}(x') = {}_0\langle G|T(\psi_\nu(x)\psi^\dagger_{\nu'}(x'))|G\rangle_0 = iG_0^{\nu\nu'}(x,x') \tag{4.8} $$

which is the *Feynman* propagator of the non-interacting system.

There is a total of six non vanishing terms that contribute to the expectation value. Each non-vanishing contribution is given by a particular way of contracting the six Fermi operators in the expectation values. The six contributions are:

1.

$$ \begin{aligned} &\frac{1}{2}\int d^4z \int d^4z' \sum_{\sigma\sigma'} V(z-z')\overbrace{\psi_\nu(x)\psi^\dagger_{\nu'}}(x')\overbrace{\psi^\dagger_\sigma(z)\psi_\sigma}(z)\overbrace{\psi^\dagger_{\sigma'}(z')\psi_{\sigma'}}(z') \\ &= \frac{1}{2}\int d^4z \int d^4z' \sum_{\sigma\sigma'} V(z-z')\left(iG_0^{\nu\nu'}(x,x')\right)\ (-iG_0^{\sigma\sigma}(z,z))\ \left(-iG_0^{\sigma'\sigma'}(z',z')\right) \end{aligned} \tag{4.9} $$

2.

$$ \begin{aligned} &\frac{1}{2}\int d^4z \int d^4z' \sum_{\sigma\sigma'} V(z-z')\overbrace{\psi_\nu(x)\psi^\dagger_{\nu'}}(x')\overbrace{\psi^\dagger_\sigma(z)\overbrace{\psi_\sigma(z)\psi^\dagger_{\sigma'}}(z')\psi_{\sigma'}}(z') \\ &= \frac{1}{2}\int d^4z \int d^4z' \sum_{\sigma\sigma'} V(z-z')\left(iG_0^{\nu\nu'}(x,x')\right)\ \left(-iG_0^{\sigma'\sigma}(z',z)\right)\ \left(iG_0^{\sigma\sigma'}(z,z')\right) \end{aligned} \tag{4.10} $$

3.

$$\frac{1}{2}\int d^4z \int d^4z' \sum_{\sigma\sigma'} V(z-z')\ \overbrace{\psi_\nu(x)\psi^\dagger_{\nu'}(x')\psi^\dagger_\sigma(z)\psi_\sigma(z)\psi^\dagger_{\sigma'}(z')\psi_{\sigma'}(z')}$$
$$= \frac{1}{2}\int d^4z \int d^4z' \sum_{\sigma\sigma'} V(z-z')\,(-iG_0^{\nu\sigma}(x,z))\ \left(-iG_0^{\sigma\nu'}(z,x')\right)\ \left(-iG_0^{\sigma'\sigma'}(z',z')\right) \tag{4.11}$$

4.

$$\frac{1}{2}\int d^4z \int d^4z' \sum_{\sigma\sigma'} V(z-z')\overbrace{\psi_\nu(x)\psi^\dagger_{\nu'}(x')\psi^\dagger_\sigma(z)\psi_\sigma(z)\psi^\dagger_{\sigma'}(z')\psi_{\sigma'}(z')}$$
$$= \frac{1}{2}\int d^4z \int d^4z' \sum_{\sigma\sigma'} V(z-z')\,(-iG_0^{\nu\sigma}(x,z))\ \left(-iG_0^{\sigma'\nu'}(z',x')\right)\ \left(iG_0^{\sigma\sigma'}(z,z')\right) \tag{4.12}$$

5.

$$\frac{1}{2}\int d^4z \int d^4z' \sum_{\sigma\sigma'} V(z-z')\overbrace{\psi_\nu(x)\psi^\dagger_{\nu'}(x')\psi^\dagger_\sigma(z)\psi_\sigma(z)\psi^\dagger_{\sigma'}(z')\psi_{\sigma'}(z')}$$
$$= \frac{1}{2}\int d^4z \int d^4z' \sum_{\sigma\sigma'} V(z-z')\left(-iG_0^{\nu\sigma'}(x,z')\right)\ \left(iG_0^{\sigma\nu'}(z,x')\right)\ \left(-iG_0^{\sigma'\sigma}(z',z)\right) \tag{4.13}$$

6.

$$\frac{1}{2}\int d^4z \int d^4z' \sum_{\sigma\sigma'} V(z-z')\overbrace{\psi_\nu(x)\psi^\dagger_{\nu'}(x')\psi^\dagger_\sigma(z)\psi_\sigma(z)\psi^\dagger_{\sigma'}(z')\psi_{\sigma'}(z')}$$
$$= \frac{1}{2}\int d^4z \int d^4z' \sum_{\sigma\sigma'} V(z-z')\left(-iG_0^{\nu\sigma'}(x,z')\right)\ (-iG_0^{\sigma\sigma}(z,z))\ \left(-iG_0^{\sigma'\nu'}(z',x')\right) \tag{4.14}$$

Hence, to lowest order in perturbation theory, *i.e. linear* in the pair interaction potential V, we get

$$
\begin{aligned}
&{}_0\langle G|\mathcal{S}|G\rangle_0\; iG_F^{\nu\nu'}(x,x') = iG_0^{\nu\nu'}(x,x')+ \\
&+\frac{1}{1!}\,\frac{(-i)}{\hbar}\,\frac{1}{2}\int dz\int dz'\;\sum_{\sigma\sigma'} V(z-z')i^3 G_0^{\nu\nu'}(x,x')G_0^{\sigma\sigma}(z,z)G_0^{\sigma'\sigma'}(z',z') && (a)\\
&+\frac{1}{1!}\,\frac{(-i)}{\hbar}\,\frac{1}{2}\int dz\int dz'\;\sum_{\sigma\sigma'} V(z-z')i^3(-1)\;G_0^{\nu\nu'}(x,x')\;G_0^{\sigma\sigma'}(z,z')G_0^{\sigma'\sigma}(z',z) && (b)\\
&+\frac{1}{1!}\,\frac{(-i)}{\hbar}\,\frac{1}{2}\int dz\int dz'\;\sum_{\sigma\sigma'} V(z-z')i^3(-1)G_0^{\nu\sigma}(x,z)G_0^{\sigma\nu'}(z,x')G_0^{\sigma'\sigma'}(z',z') && (c)\\
&+\frac{1}{1!}\,\frac{(-i)}{\hbar}\,\frac{1}{2}\int dz\int dz'\;\sum_{\sigma\sigma'} V(z-z')i^3 G_0^{\nu\sigma}(x,z)G_0^{\sigma'\nu'}(z',x')G_0^{\sigma\sigma'}(z,z') && (d)\\
&+\frac{1}{1!}\,\frac{(-i)}{\hbar}\,\frac{1}{2}\int dz\int dz'\;\sum_{\sigma\sigma'} V(z-z')i^3 G_0^{\nu\sigma'}(x,z')G_0^{\sigma'\sigma}(z',z)G_0^{\sigma\nu'}(z,x') && (e)\\
&+\frac{1}{1!}\,\frac{(-i)}{\hbar}\,\frac{1}{2}\int dz\int dz'\;\sum_{\sigma\sigma'} V(z-z')i^3(-1)G_0^{\nu\sigma'}(x,z')G_0^{\sigma'\nu'}(z',y)G^0_{\sigma\sigma}(z,z) && (f)\\
&\qquad\qquad +\ldots && (4.15)
\end{aligned}
$$

We will use Feynman diagrams to do the bookkeeping for us. Thus to each factor of $iG_0^{\nu\nu'}(x,x')$ we associate an oriented line running from x to x', as shown in Fig.4.2(a). The line is oriented since the state created (or destroyed) by the field operator is either an electron or a hole, which both charged. Thus the orientation of the propagator lines follows from charge conservation. Similarly, each interaction is given in terms of the potential $V(x-x')$, which we will call a *vertex* and it is shown in Fig.4.2(b). In this case the vertex is spin-independent but in other cases , *e.g.* exchange interactions, the vertex has a non-trivial spin structure.

We will now assign a Feynman diagram to each contribution in Eq.(4.15). Let us consider the first contribution to Eq.(4.15), which we have denoted by (a). In this term

- There are two external points, x and x' (and their spin labels ν and ν'), and (in this case) one pair of internal points, z and z' (and the internal spin labels σ and σ').
- there is an interaction factor of $\frac{1}{2}V(z-z')$, which in this case is spin-independent

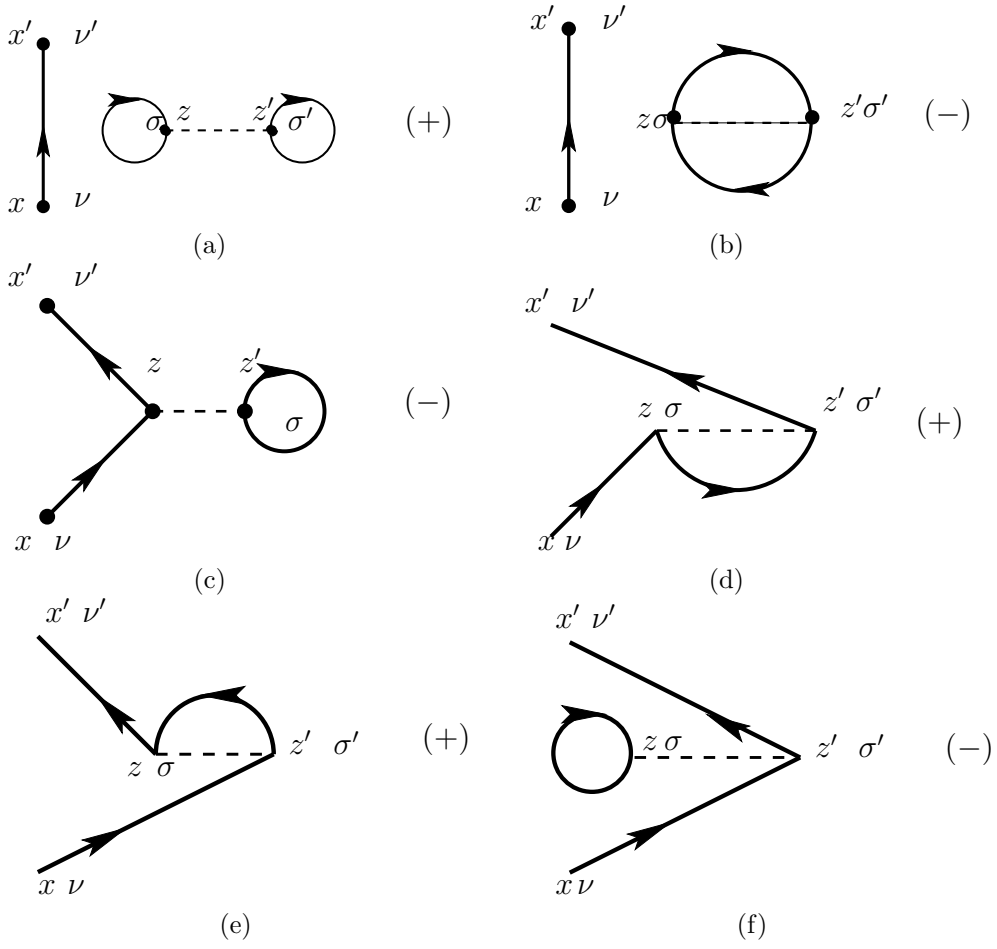

Figure 4.1: Feynman diagrams for the first order contributions to the electron propagator, Eq.(4.15); the contributions of the diagrams (d) and (e) are equal, and so are the diagrams (c) and (f). The $(\pm)$ signs denote the fermionic sign of the diagram.

(a) Propagator (b) Vertex

Figure 4.2: Feynman rules

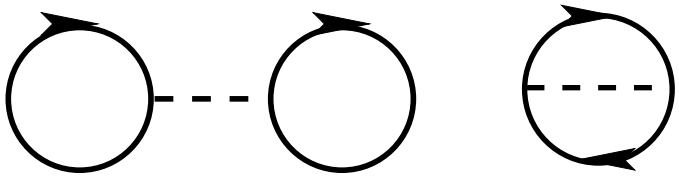

Figure 4.3: Vacuum Diagrams

- There is a sum over the internal spin labels and integrals over the internal space-time coordinates
- there is an overall factor of $\frac{1}{1!}\left(\frac{-i}{\hbar}\right)$.
- There are three operator contractions, and each contraction is a factor of i multiplying a Feynman propagator.
- The contractions link the external points x and x' (and their spin labels ν and ν') to each other and to the internal points z and z' (and to the internal spin labels σ and σ').
- There is an overall sign that results from the anticommutation rules

We will draw a Feynman diagram for this contribution by drawing an oriented line for each contraction. These three lines connect the external points x and x' to each other and to the internal coordinates z and z'. We will draw a broken line connecting the coordinates z and z'. The spin labels must also be contracted to each other as in this theory the propagators are diagonal in spin. The result is shown in Fig.4.1(a).

Notice that in this contribution the external points are contracted to each other and that the internal points are connected to each other but not to the external points. This is an example of a *disconnected diagram*: this diagram can be split in two separate pieces (each corresponding to a separate factor in the actual expression) by drawing a line that does not cross (or cut) any propagator line. In fact, the wto factor are just a free propagator factor $iG_0^{\nu\nu'}(x,x')$ and a diagram obtained by contracting only the internal vertices (the two loops in Fig.4.1(a)).

This factor also shows up in the perturbative expansion of the denominator ${}_0\langle G|\mathcal{S}|G\rangle_0$:

$$\langle G|\mathcal{S}|G\rangle = 1 + \left(\frac{-i}{\hbar}\right)\left\{\frac{1}{2}\int_{zz'} V(z-z')\, G^0_{\sigma\sigma}(z,z)G^0_{\sigma'\sigma'}(z',z') + \frac{1}{2}\int_{zz'} V(z-z')(-1)G^0_{\sigma\sigma'}(z,z')G^0_{\sigma'\sigma}(z',z)\right\} + \ldots$$

$\equiv 1 +$ 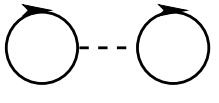 $+\ldots$ (4.16)

which have a diagrammatic for shown in Fig.4.3.

We can now assign a diagram to each of the contributions to Eq.(4.15) and Eq.(4.16). The corresponding diagrams are shown in Fig.4.1(b)-(f), and in Fig.4.3(a) and (b).

We now notice that we can write (in compact form)

${}_0\langle G|\mathcal{S}|G\rangle_0\, iG_F = iG_F \left\{1 +\right.$ 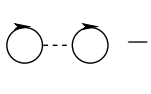 $\left.+\ldots\right\}$

$=$ 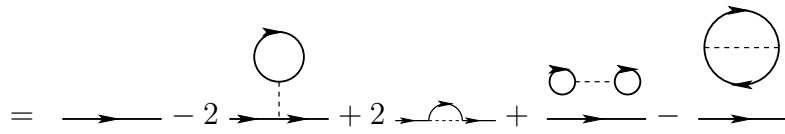

$= \left\{\right.$ 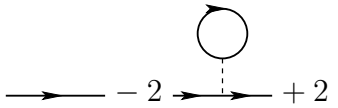 $\left.+\ldots\right\}\left\{1 +\right.$ 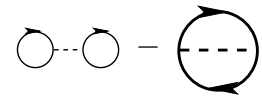 $\left.+\ldots\right\}$ (4.17)

Hence, the disconnected diagrams are canceled exactly by the denominator ${}_0\langle G|S|G\rangle_0$ (the "vacuum graphs"). This result is true to all orders in perturbation theory. Thus when calculating a Green's function we only need to calculate *connected diagrams*. To first order in perturbation theory, we

find that the electron Green function, the Feynman propagator, is

$iG_F(x,x') =$ 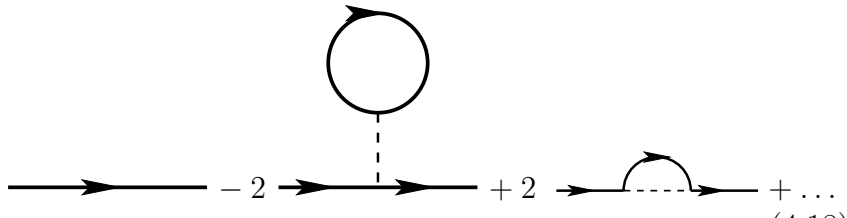 $+\ldots$ (4.18)

The two leading perturbative contributions are the Hartree term (the second term above) and the Fock term (the third term.) Notice that the term with one fermion loop has a negative sign.[1]

We will now summarize the *Feynman Rules* (in position space) for a fermion N-point function, which has N external legs (attached to the N external points). The Feynman diagrams for an n-th order contribution in perturbation theory are obtained as follows:

1. Pair up all vertices (internal and external) one with an outgoing arrow to one with an incoming arrow

2. Assign a contraction to each pair and a factor of iG_0 to each.

3. Weight of the diagram:

$$\frac{1}{n!}\left(\frac{-i}{\hbar}\right)^n \prod_{j,k=1}^{n} V(z_j - z_k) \times \text{ products of factors of } iG_0 \qquad (4.19)$$

4. Assign a factor of $(-1)^F$ where F is the number of fermionic loops in the diagram

5. Integrate over space-time coordinates of internal vertices

6. Sum over all internal (contracted) spin labels

7. Consider only connected diagrams.

[1]The factors of 2 come about because that interaction is non-local. These factors cancel against the factors of 1/2 of the interaction mediated by the pair potential. With this in mind we will drop both factors and count each diagram only once.

4.2 Effective interaction and Screening

We can calculate the effective interaction by calculating the density-density correlation function (or density propagator)

$$\begin{aligned}\Pi(x,x') &= -\frac{i}{\hbar}\langle G|T(n(x)n(x'))|G\rangle \\ &= -\frac{i}{\hbar}\sum_{\sigma\sigma'}\langle G|T\psi^\dagger_\sigma(x)\psi_\sigma(x)\psi^\dagger_{\sigma'}(x')\ \psi_{\sigma'}(x')|G\rangle \end{aligned} \tag{4.20}$$

To zeroth-order in perturbation theory, *i.e.* in the absence of interactions, we can compute this expectation value by using Wick's Theorem:

$$\Pi_0(x,x') = -\frac{i}{\hbar}\sum_{\sigma\sigma'}\left\{\overbrace{\psi^\dagger_\sigma(x)\psi_\sigma}(x)\overbrace{\psi^\dagger_{\sigma'}(x')\psi_{\sigma'}}(x') + \overbrace{\psi^\dagger_\sigma(x)\overbrace{\psi_\sigma(x)\psi^\dagger_{\sigma'}}(x')\psi_{\sigma'}(x')}\right\} \tag{4.21}$$

Hence we get

$$\begin{aligned}\Pi_0(x,x') &= \left(\frac{-i}{\hbar}\right)\ \left\{{}_0\langle G|n(x)|G\rangle_{00}\langle G|n(x')|G\rangle_0\ + \mathrm{tr}\ \left(G_0(x,x')G^0(x',x)\right)\right\} \\ &\equiv \left(\frac{-i}{\hbar}\right)\left\{\rho^2 + \mathrm{tr}\ G_0(x,x')G_0(x',x)\right\} \\ &\equiv \frac{-i}{\hbar}\ \rho^2 + \Pi^0_c(x,x')\end{aligned} \tag{4.22}$$

where we have introduced the *connected* density-density correlation function

$$\Pi^0_c(x,x') = -\frac{i}{\hbar}\ \mathrm{tr}\ [\ G_0(x,x')G_0(x',x)\ ] \tag{4.23}$$

We will consider now the *connected two particle Green function* (or 4-point function)

$$G^{(2)}_c(x_1\sigma_1;x_2\sigma_2;x_3\sigma_3,x_4\sigma_4) = \langle G|T\psi(1)\psi(2)\psi^\dagger(3)\psi^\dagger(4)|G\rangle_c \tag{4.24}$$

where we have denoted by $k = 1,2,3,4$, both the space-time coordinate x_k *and* the spin label σ_k. To zeroth order in perturbation theory there are no connected pieces since both non-vanishing contributions to this expectation

value factorize:

$$\overbrace{\psi(1)\psi(2)\psi^\dagger(3)\psi^\dagger(4)} + \overbrace{\psi(1)\psi(2)\psi^\dagger(3)\psi^\dagger(4)} \;=\; iG_0(1,4)\; iG_0(2,3) - iG_0(1,3)\; iG_0(2,4)$$

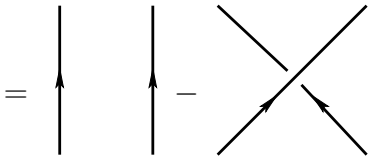

(4.25)

The first disconnected contribution is known as the *direct* term, while the second disconnected contribution is known as the *exchange* term.

The first *connected* contribution to the two-particle Green function (or 4-point function) appears in first order in perturbation theory, whose contribution to the two-particle Green function is

$$\left(\frac{-i}{\hbar}\right)\;\frac{1}{2}\;\int dz_1 \int dz_2 \sum_{\alpha_1\alpha_2} V(z_1-z_2) \times {}_0\langle G|T\psi_{\sigma_1}(x_1)\psi_{\sigma_2}(x_2)\psi^\dagger_{\sigma_3}(x_3)\psi^\dagger_{\sigma_4}(x_4)\psi^\dagger_{\alpha_1}(z_1)\psi_{\alpha_1}(z_1)\psi^\dagger_{\alpha_2}(z_2)\psi_{\alpha_2}(z_2)|G\rangle_0 \tag{4.26}$$

Again, considering only connected pieces and ignoring vacuum diagrams (which cancel out exactly), we find that to lowest order in perturbation theory the connected two-particle Green function is given by two fully connected (and identical) contributions[2]

$$G_c^{(2)}(1,2;3,4) \;=\;$$

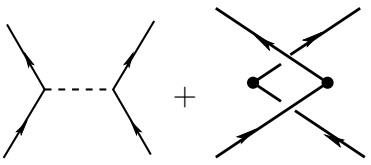

$$+\ldots$$

$$= \left(\frac{-i}{\hbar}\right)\;\frac{2}{2}\int dz_1 \int dz_2 V(z_1-z_2)\; iG_0(1,z_1)iG_0(2,z_2)iG_0(z_2,3)iG_0(z,4) + \ldots \tag{4.27}$$

Thus, is we ignore the contributions from the external legs $G_c^{(2)}$, we see that the connected two-particle Green function $G_c(1,2;3,4)_c$ is just the interaction

[2]Notice again the cancelation of the factors of 1/2.

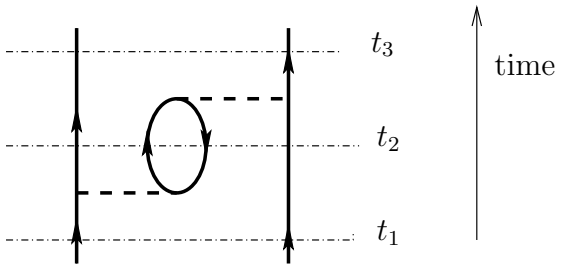

Figure 4.4: Intermediate states with particle-hole pairs in two-particle scattering processes

potential. This is then a way to measure the *effective interactions* in the system including screening the electrons!

What happens at higher orders in perturbation theory? The lowest order contributions schematically look as follows:

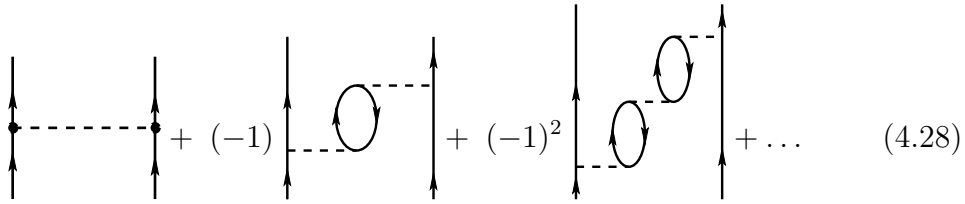

(4.28)

Let's examine this a little closer. Let us consider that we act on the ground state by removing two electrons (or creating two holes) and that in the final state we also have two holes. Then, to second order in perturbation theory, the interaction can mix this state with an intermediate state in which there is an extra particle-hole pair in the intermediate state. This is shown in Fig.4.4.

In higher orders we will have processes, among others, which in the intermediate states have, in addition to the two incoming particles (or holes), a number of particle-hole pairs. There are also processes, shown in Fig.4.5, in which two particles (or two holes) scatter each into intermediate states without additional particle-hole pairs.

However we notice that there are higher order terms which consist basically in stringing together diagrams that include one fermion loop, one after each other, as in Fig. 4.6 (a) and (b). These sum over all of these diagrams can be viewed as an effective interaction.

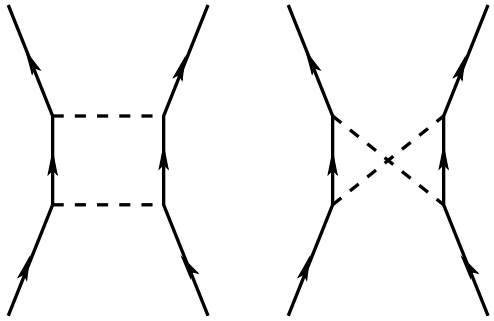

Figure 4.5: Processes not included in RPA

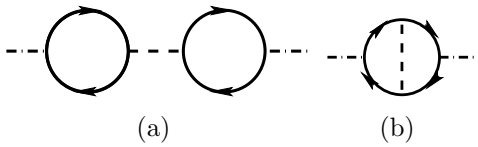

Figure 4.6: Two-loop bubble diagrams

This motivates us to consider the sum over all such processes, leading to an *effective interaction* $V_{\text{eff}}(z - z')$, which is no longer instantaneous. When the intermediate process is represented by an elementary bubble diagram, Fig.4.7, one obtains an approximate form of the effective interaction known as the *Random Phase Approximation*, which is asymptotically exact in the high density limit (see below).

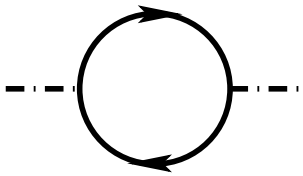

Figure 4.7: One-loop bubble diagram

We will now sum over all these *bubble diagrams*. The n-th order term comes in $n!$ copies which are just permutations an thus leads to an overall

factor of $n!$. We will do the sum by amputating the external legs (propagators) from each diagram. We find

$$V_{\rm eff}(z-z') = V(z-z') + \frac{1}{2!}\int d1d2V(z-1)\ \Pi_c^0(1,2)V(2-z') \\ +\frac{1}{2!}\ 2!\int d1d2\int d1'd2'V(z-1)\Pi_c^0(1,1')V(1'-2')\Pi_c^0(2',2)V(2-z') \\ +\ldots \tag{4.29}$$

where we have used $\Pi_c^0(x,x')$, the connected density-density correlation function of the non-interacting system, defined in Eq.(4.23).

Hence the effective interaction is the solution of the integral equation

$$\boxed{V_{\rm eff}(x_1-x_2) = V(x_1-x_2) + \int dz_1\int dz_2\ V(x_1-z_1)\ \Pi_c^0(z_1,z_2)V_{\rm eff}(z_2-x_2)} \tag{4.30}$$

We will see that in momentum space it is quite easy to solve this equation.

4.3 Feynman Rules in Momentum Space

We will now discuss briefly the Feynman rules in momentum space. Let us begin by recalling the form of the Hamiltonian in momentum space. The non-interacting Hamiltonian $H_0 \equiv H_0 - \mu N$ is simply

$$H_0 = \int \frac{d^3p}{(2\pi\hbar)^3}\sum_\sigma E(\vec{p})\ \psi_\sigma^\dagger(\vec{p})\psi_\sigma(\vec{p}) \tag{4.31}$$

where $E(\vec{p})$ is the excitation energy measured from the Fermi energy E_F,

$$E(\vec{p}) \equiv \frac{\vec{p}^{\,2}}{2m} - E_F \tag{4.32}$$

The interaction term H_1 is

$$H_1 = \frac{1}{2}\int\frac{d^3p}{(2\pi\hbar)^3}\int\frac{d^3q}{(2\pi\hbar)^3}\int\frac{d^3}{(2\pi\hbar)^3}\sum_{\sigma,\nu=\uparrow,\downarrow}\widetilde{V}(\vec{k})\ \psi_\sigma^\dagger(\vec{p}+\vec{k})\psi_\nu^\dagger(\vec{q}-\vec{k})\psi_\nu(\vec{q})\psi_\sigma(\vec{p}) \tag{4.33}$$

where $\widetilde{V}(\vec{k})$ is the Fourier transform of the two-particle interaction potential

$$\widetilde{V}(\vec{k}) = \int d^3x \; V(\vec{x}) \; e^{-i\vec{k} \cdot \vec{x}/\hbar} \tag{4.34}$$

Recall that for the Coulomb interaction in three dimensions $\widetilde{V}(\vec{k})$ is

$$\widetilde{V}(\vec{k}) = \frac{4\pi e^2 \hbar^2}{\varepsilon_0 \mid \vec{p} \mid^2} \tag{4.35}$$

where ε_0 is the dielectric constant of the background medium in which the electrons move.

Similarly, the Fourier transform (in space and time) of the Feynman propagator

$$G_0^{\sigma\sigma'}(\vec{x}-\vec{x}\,', t-t') = \int \frac{d\omega}{2\pi\hbar} \int \frac{d^3p}{(2\pi\hbar)^3} \; e^{i\vec{p} \cdot (\vec{x}-\vec{x}\,')/\hbar} e^{-i\omega(t-t')/\hbar} \; G_0^{\sigma\sigma'}(\vec{p},\omega) \tag{4.36}$$

where

$$\begin{aligned} G_0^{\sigma\sigma'}(\vec{p},\omega) &= \delta_{\sigma\sigma'} \left[\frac{\theta(\mid \vec{p} \mid - p_F)}{\omega - \frac{E(p)}{\hbar} + i\delta} + \frac{\theta(p_F - \mid \vec{p} \mid)}{\omega - \frac{E(\vec{p})}{\hbar} - i\delta} \right] \\ &\equiv \frac{\delta_{\sigma\sigma'}}{\omega - \frac{E(p)}{\hbar} + i \; \mathrm{sign}(\mid p \mid - p_F) \; \delta} \end{aligned} \tag{4.37}$$

On the other hand, since $E(\vec{p}) = \frac{\vec{p}^{\,2}}{2m} - E_F > 0$ for $\mid \vec{p} \mid > p_F$ and viceversa, we can also write the propagators as

$$G_0^{\sigma\sigma'}(\vec{p},\omega) = \frac{\delta_{\sigma\sigma'}}{\omega - \frac{E(p)}{\hbar} + i \; \mathrm{sign}(\omega) \; \delta} \equiv \delta_{\sigma\sigma'} G_0(p) \tag{4.38}$$

Thus, for $\omega < 0$ (*i.e.* below the Fermi energy) the unperturbed Feynman propagator $G_0(\omega, \vec{p})$ has poles on the *upper* half of the complex frequency plane (corresponding to *holes*) while for $\omega > 0$ (*i.e.* above the Fermi energy) it has poles on the *lower* half of the complex frequency plane, as shown in Fig.4.8. There is a pole on the real axis for each momentum $\vec{p}$ (and spin projection) at $E(\vec{p})/\hbar$. The distance between poles vanishes in the thermodynamic limit: the poles coalesce into a *branch cut*. This is characteristic of a Fermi system without an energy gap.

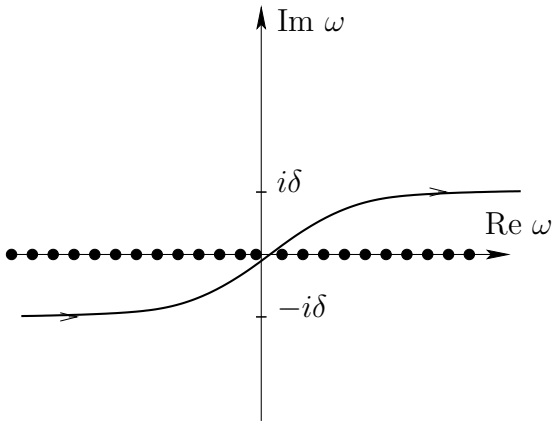

Figure 4.8: Singularities of the Electron Feynman propagator on the complex frequency plane. The "bullets" are the poles for the single-particle state of momentum $\vec{p}$.

The Feynman rules in momentum space are the essentially same as in position space except that now we have to ensure that energy and momentum is conserved at every interaction vertex. Thus given any diagram in the position space representation well can always use a Fourier transform to get the momentum space representation. (In what follows we will use the notation $p = (\omega, \vec{p})$). Thus the rules now are

- every fermion line carries energy momentum p
- every interaction line carries a momentum transfer q
- every fermion contraction is a factor of $iG_0(p)$
- every interaction with momentum transfer q is a factor $\widetilde{V}(q)$ energy and momentum must be conserved at every vertex.

(a) (b)

Figure 4.9: (a) $G_0^{\sigma\sigma'}(p)$; (b) $V(q)$.

- there is a factor of $(-1)F$ for a diagram with F fermion loops
- internal momenta and spin labels must be integrated and summed over
- there is the same factor of $1/n!$ and $(-i/\hbar)^n$ to order n in perturbation theory

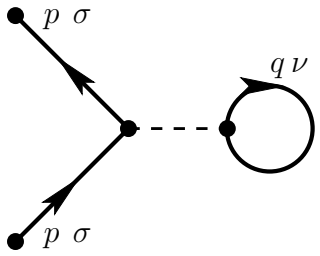

For example, the Feynman diagram shown in Eq.(4.1)(c), which in momentum space is shown in Fig.4.3, in momentum space represents the following contribution to the propagator

$$\delta G^{\sigma\sigma'}_{(1)}(p) \;= \left(\frac{-i}{\hbar}\right) 2\delta_{\sigma\sigma'}\; G_0(p)G_0(p)\widetilde{V}(0)\int_q G_0(q) \tag{4.39}$$

where

$$\widetilde{V}(0) = \lim_{q\to 0}\widetilde{V}(q) \tag{4.40}$$

and the overall factor of 2 is due to the spin trace in the internal fermion loop.

Note that, although for the case of Coulomb interactions

$$\lim_{q\to 0}\widetilde{V}(q) = \infty \tag{4.41}$$

if we include the effects of the neutralizing positive background charge of the ions, which amounts to to subtract the average charge density from the local electronic density operator $\rho(x)$ (or, equivalently, to *normal order* the density operator), this term divergent term exactly cancels out.

As another example we will consider the one loop correction to the two-particle scattering process shown in Fig.4.10, which yields the expression:

$$\delta_{\sigma\sigma'}\delta_{\nu\nu'}2\times 2(-1)\frac{1}{2!}\left(\frac{-i}{\hbar}\right)^2 G_0(p)G_0(p+k)G_0(p')G_0(p'-k)\left[\widetilde{V}(k)\right]^2\int_q G_0(q)G_0(k+q) \tag{4.42}$$

Here, one factor of 2 in front is the spin contribution from the internal fermion loop; the second factor of 2 comes from the topologically in-equivalent diagram.

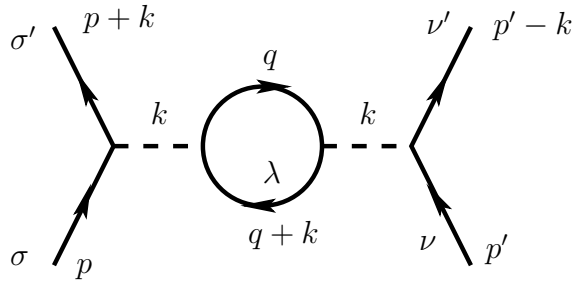

Figure 4.10: One loop correction in momentum space

4.4 The Dyson Equation and The Self Energy

The structure of the equation for the effective interaction $V_{\rm eff}$, eq.(4.30), is quite generic. The quantity we called Π_c^0 is just the leading correction to the *polarization function*. In momentum space, Eq.(4.30) becomes

$$V_{\rm eff}(k) = V(k) + V(k)\Pi(k)V_{\rm eff}(k) \tag{4.43}$$

In Eq.(4.30), $\Pi(k)$ is just $\Pi_c^0(k)$ to lowest order in perturbation theory.

Eq.(4.30) (and Eq.(4.74)) is an example of a *Dyson Equation* and the quantity $\Pi(k)$ is a *self-energy*. In terms of $\Pi(k)$, the explicit solution of Eq.(4.74) is

$$V_{\rm eff}(k) = \frac{V(k)}{1 - V(k)\Pi(k)} \tag{4.44}$$

We will shortly analyze the behavior of $V_{\rm eff}(k)$.

The (connected) density-density correlation function $\mathcal{D}_{00}(p,\omega) \equiv \Pi_c(p,\omega)$(can also be computed within this (RPA) approximation. Indeed we saw that, to zeroth-order in perturbation theory, it is just $\Pi_0^c(p,\omega)$. Within RPA it is replaced by the bubble sum:

$$\Pi_c(p,\omega) = \Pi_c^0(p,\omega) + \Pi_c^0(p,\omega)V(k)\Pi_c(p,\omega) \tag{4.45}$$

or,what is the same

$$\Pi_c(p,\omega) = \frac{\Pi_c^0(p,\omega)}{1 - V(k)\Pi_c(p,\omega)} \tag{4.46}$$

This result already tells us, at this lowest order of approximation, what is the *induced charge density* $\rho^{\rm ind}(p,\omega)$ due to an external perturbation due to a static external charge which interacts with the scalar potential $V(p,\omega)$ (the Fourier transform of the Coulomb potential). We find

$$\langle \rho^{\rm ind}(p,\omega)\rangle = \Pi_c(p,\omega)V(p,\omega) = \Pi_c^0(p,\omega)V_{\rm eff}(p,\omega) = \frac{V(p,\omega)\Pi_c^0(p,\omega)}{1 - V(p,\omega)\Pi_c^0(p,\omega)} \tag{4.47}$$

For a *static* probe, the potential is independent of time and and hence the frequency has to be set to zero, $\omega \to 0$. We will see in the next section what this implies in an explicit computation.

The same analysis can be applied to the Fermion Green Function. In momentum space, $G_F(k)$ has the perturbative expansion

$G_F(p)$ =

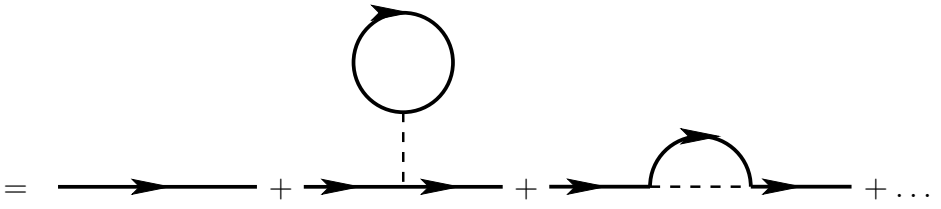

(4.48)

In higher orders in perturbation theory we will find diagrams such as those of Fig.4.11(a) and (b). In Fig.4.11 we see that there are two types of diagrams: (a) diagrams that can be split in two by cutting a single propagator line *inside* the diagram (carrying the external momentum p), and (b) diagrams that *cannot* be split in two by cutting a single internal propagator line. The first type of diagrams are said to be *one-particle reducible*; the second type of diagrams are *one-particle irreducible*. It is easy to see that summing all the *one-particle reducible* diagrams of *all types* lead us to rewriting the perturbation series as

(4.49)

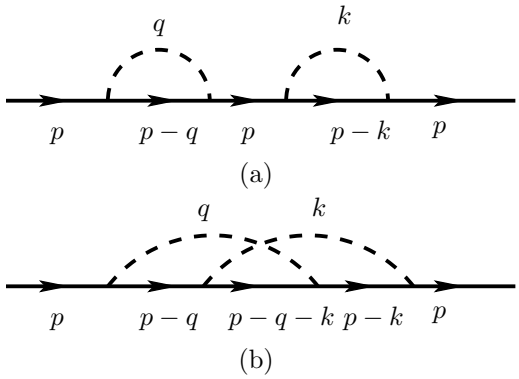

Figure 4.11: One-particle reducible (a) and irreducible (b) Feynman diagrams.

which is known as the Dyson equation for the full Feynman propagator. Here the filled "blob", which we will cal the *self energy*, is the sum of all *one-particle irreducible* diagrams (upon amputating their external legs).

The Dyson equation which has the explicit form

$$G_F^{\sigma\sigma'}(k) = G_0^{\sigma\sigma'}(k) \; + \; G_0^{\sigma\nu}(k)\, \Sigma^{\nu\nu'}(k)\, G_F^{\nu'\sigma'}(k) \tag{4.50}$$

where $\Sigma^{\nu\nu'}(k)$ is the self energy operator. The formal solution of the Dyson equation is

$$\left(G^{-1}(k)\right)^{\sigma\sigma'} \; = \; G_0(k)^{\sigma\sigma'} - \left(\Sigma^{-1}(k)\right)^{\nu\nu'} \tag{4.51}$$

In a paramagnetic metal, the ground state is spin unpolarized. Thus G_0 and G_F must be independent of the spin polarization, and G_0, G_F and the self energy Σ have the form

$$G_0^{\sigma\sigma'}(k) = \; \delta_{\sigma\sigma'}\, G_0(k), \quad G_F^{\sigma\sigma'}(k) = \delta_{\sigma\sigma'} G_F(k), \quad \Sigma^{\sigma\sigma'}(k) \; = \; \delta_{\sigma\sigma'}\, \Sigma(k) \tag{4.52}$$

where

$$G_F^{-1}(k) = G_0^{-1}(k) - \Sigma(k) \tag{4.53}$$

The self-energy $\Sigma(k)$ can be split into its real and imaginary parts

$$\Sigma(k) \; = \Sigma'(k) + i\, \Sigma''(k) \tag{4.54}$$

Since $G_F(k)$ is the (full) Feynman propagator, the imaginary part of the self energy obeys

$$\text{sign}\; \Sigma''(k) \; = \; -\text{sign}\left(\mid \vec{k} \mid - p_F \right) \tag{4.55}$$

Since the free propagator obeys

$$G_0^{-1}(k) \;=\; \omega - E_0(k) + i\delta \,\mathrm{sign}\left(\mid \vec{k} \mid -p_F\right) \tag{4.56}$$

where $E_0(k) = \dfrac{\vec{k}^{\,2}}{2m} - E_F$ is the free particle spectrum, the full propagator $G_F(k)$ must obey

$$\begin{aligned} \mathrm{Re}\, G^{-1}(k) &= \omega - E_0(k) - \Sigma'(k) \\ \mathrm{Im}\, G^{-1}(k) &= (\delta - \mid \Sigma''(k) \mid) \,\mathrm{sign}\left(\mid \vec{k} \mid -p_F\right) \end{aligned} \tag{4.57}$$

Now, if $\lim \Sigma''(k) \nrightarrow 0$, then the poles of the full propagator move away from the real axis. The poles of $G_F(k)$ are the *quasiparticles* of the fully interacting system. Hence, if the poles move away from the real axis, this means that the *quasiparticle* states are not necessarily sharp in energy and have a finite width, or what is equivalent, $\Sigma''(k)$ is the *quasiparticle decay rate* and $\Sigma''(k)^{-1}$ is the *quasiparticle lifetime*. Moreover, the equation for zeros of the real part of $G_F(k)^{-1}$

$$\omega(\vec{k}) - E_0(k) - \Sigma'(\omega(\vec{k}), \vec{k}) = 0 \tag{4.58}$$

define the *effective quasiparticle dispersion*. In the non-interacting case, for $\mid \vec{k} \mid$ close enough to the Fermi momentum p_F, and for energies close enough to the Fermi surface, $\omega \to 0$, we can use a linearized spectrum

$$E_0(\vec{k}) \cong v_F(|\vec{k}| - p_F) \tag{4.59}$$

where v_F is the Fermi velocity

$$\vec{v}_F = \left.\frac{\partial E_0}{\partial \vec{k}}\right|_{p_F} \tag{4.60}$$

Only a momentum change in the direction *normal* to the Fermi surface costs energy. The imaginary part of $\Sigma''(k)$ is the width of the quasiparticle state at momentum $\vec{k}$.

However, the quasiparticles are physically meaningful only if they are stable, *i..e* if they are long lived. Thus, there must be restrictions on the allowed behavior of $\Sigma''(k)$ for the quasiparticles to remain stable even after

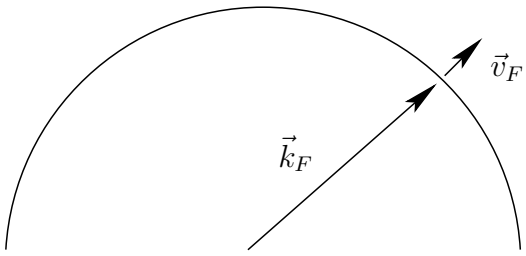

Figure 4.12: The Fermi surface

interactions are taken into account. Physically we expect that a very energetic quasiparticle can decay into a collection of quasiparticles and quasiholes and thus that there should be a finite width at finite frequency ω. However, for the *low-energy excitations* this cannot be the case since otherwise would would have to conclude that the perturbed electron gas would be completely different than the free Fermi gas. We will see that, in a certain limit that we will discuss later, the interacting Fermi gas can behave much in the same way as the non-interacting Fermi gas (up to important corrections). This is the basis of the Landau Theory of the Fermi Liquid. However we will see that in some cases, such as in one space dimension, this picture breaks down even for infinitesimally weak interactions. This is the case of the 1D Luttinger liquid.

Hence, the quasiparticles are stable provided

$$\lim_{\omega \to 0} \Sigma''(\vec{k}, \omega) = 0 \tag{4.61}$$

However, since the real part also vanishes, *linearly*, as the Fermi surface is approached, the quasiparticles can remain sharply defined states only is Σ'' vanishes *faster than linear* as $\omega \to 0$. If we assume that the frequency dependence of Σ'' is *analytic*, then a behavior $\Sigma'' \sim \omega^2$ as $\omega \to 0$ and $|\vec{k}| \to p_F$ is consistent with the stability of the quasiparticles. This is the behavior found in the weakly interacting electron gas, and it is the key assumption of the *Landau Theory of the Fermi Liquid*, which we will discuss shortly.

In particular, this arguments also imply that in the asymptotic low energy regime the behavior full Green function is be dominated by the pole. Hence at low energies the full propagator G_F must have a *singular part* $G_{\rm sing}(\vec{k}, \omega)$, dominated by the pole, and a *regular part*

$$G_F(\vec{k}, \omega) = G_{\rm sing}(\vec{k}, \omega) + G_{\rm reg}(\vec{k}, \omega) \tag{4.62}$$

where

$$G_{\rm sing}(\vec{k},\omega) = \frac{Z(\vec{k},\omega)}{\omega - \left(\left|\vec{k}\cdot\vec{v}_F\right| - p_F\right) + i\ {\rm sign}\omega\ \delta} \tag{4.63}$$

which holds asymptotically for $\omega \to 0$ and $\mid \vec{k} \mid \to p_F$. The quantity

$$\lim_{\omega\to 0}\lim_{|\vec{k}|\to p_F} Z(\vec{k},\omega) \equiv Z \tag{4.64}$$

is called the *residue*, which turns out to have the bounds

$$0 < Z \leq 1 \tag{4.65}$$

What does the residue mean physically? Recall that the definition of the propagator

$$G_F(x-x') = i\langle G|T(\psi(x)\psi^\dagger(x'))|G\rangle \tag{4.66}$$

As $t-t' \to \infty$, the propagator measures the amplitude that a state prepared in the remote past by acting on the ground state $|G\rangle$ with the *electron operator* $\psi^\dagger(x')$ will evolve into the same state in the remote future. In momentum space, this will be an initial state with one *bare electron* with momentum $|\vec{p}\rangle$ and we are asking for the overlap with the actual exact eigenstate of H which mixes with the bare electron state. The residue Z at the Fermi surface is precisely this overlap. Thus if Z is close to 1 the exact state will not differ much from the bare state but as Z becomes very small the states will become increasingly different. In the limit $Z \to 0$ the eigenstates are *orthogonal* to the bare electron and the whole framework breaks down. As we will see this is what happens generically in one-dimensional systems. We will also see below that the regular part $G_{\rm reg}(\vec{k},\omega)$ represents a *continuum* of multi-quasiparticle processes.

Let us discuss the behavior of the *occupation number*

$$n(\vec{k}) = \langle G|\psi^\dagger_\sigma(\vec{k})\psi_\sigma(\vec{k})|G\rangle \tag{4.67}$$

in an interacting system:

$$\langle G|n(\vec{k})|G\rangle = -i\lim_{t'\to t^+} {\rm tr}\ G_F(\vec{k},t;\vec{k},t') = -i\int_{-\infty}^{\infty}\frac{d\omega}{2\pi\hbar}{\rm tr}\ G_F(\vec{k},\omega) \tag{4.68}$$

From the form of the singular part of the propagator, Eq.(4.63), we see that this expectation value has a *jump* or *discontinuity* at the Fermi surface

$${\rm disc.}\left\{\langle G|n(\vec{k})|G\rangle\right\} = \lim_{\omega\to 0}\lim_{|\vec{k}|\to p_F} Z(\vec{k},\omega(\vec{k})) \equiv Z \leq 1 \tag{4.69}$$

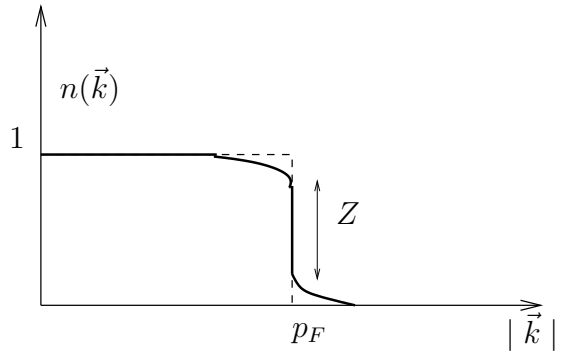

Figure 4.13: Discontinuity in the occupation number at the Fermi surface in an interacting system. The dotted line is the behavior of the non-interacting Fermi system.

Thus, the quasiparticle picture is consistent if there is a jump in the occupation number at the Fermi surface.[3]

4.5 The Dielectric Function

We will now return to the calculation of the effective interaction, Eq.(4.30), which is easy to solve in momentum space. Let

$$V(z) = \int \frac{d^4k}{(2\pi\hbar)^4}\, \widetilde{V}(k)\, e^{ik\cdot z}, \qquad kz = \frac{\vec{k}\cdot\vec{z}}{\hbar} - \omega t \tag{4.70}$$

and

$$\Pi_c^0(x-x') = \int \frac{d^4k}{(2\pi\hbar)^4}\, \widetilde{\Pi}_c^0(k)\, e^{ik\cdot(x-x')} \tag{4.71}$$

[3]The actual value of the fermi energy and of the Fermi momentum change as a result of the interactions.

Since $V(z) = V(\vec{z})\delta(t)$, its Fourier transform $\widetilde{V}(k) = \widetilde{V}(\vec{k})$ is independent of the frequency ω. Also, since

$$\int dx_1^4 dx_2^4 \, V(z - x_1) \, \Pi_c^0(x_1 - x_2) \, V_{\text{eff}}(x_2 - z') =$$

$$\int \frac{d^4k}{(2\pi\hbar)^4} \int \frac{d^4p}{(2\pi\hbar)^4} \int \frac{d^4p'}{(2\pi\hbar)^4} \, \widetilde{\Pi}_c^0(k) \, \widetilde{V}(p) \, \widetilde{V_{\text{eff}}}(p')$$

$$\times \; (2\pi\hbar)^4 \delta^4(-p + k)(2\pi\hbar)^4 \delta^4(-k + p') \, e^{i(pz - p'z')} \tag{4.72}$$

$$= \int \frac{d^4k}{(2\pi\hbar)^4} \, \widetilde{V}(k) \, \widetilde{\Pi}_c^0(k) \, \widetilde{V_{\text{eff}}}(k) \, e^{ik(z - z')} \tag{4.73}$$

which leads to the momentum-space form of the Dyson equation for the effective interaction, Eq.(4.30):

$$\widetilde{V_{\text{eff}}}(k) = \widetilde{V}(k) + \widetilde{V}(k) \, \widetilde{\Pi}_c^0(k) \, \widetilde{V_{\text{eff}}}(k) \tag{4.74}$$

The solution of Eq.(4.74) is

$$\widetilde{V_{\text{eff}}}(\vec{k}, \omega) = \frac{\widetilde{V}(\vec{k})}{1 - \widetilde{V}(\vec{k}) \, \widetilde{\Pi}_c^0(\vec{k}, \omega)} \equiv \frac{\widetilde{V}(\vec{k})}{\varepsilon(\vec{k}, \omega)} \tag{4.75}$$

where we introduced the *dielectric function* $\varepsilon(\vec{k}, \omega)$. Recall that for Coulomb interactions $V(R) = \dfrac{e^2}{\varepsilon_0 R}$ and $\widetilde{V}(\vec{k}) = \dfrac{4\pi\hbar^2 e^2}{\varepsilon_0 \vec{k}^{\,2}}$. Hence, the effective interaction becomes

$$\widetilde{V_{\text{eff}}}(\vec{k}, \omega) = \frac{4\pi\hbar^2 e^2}{\varepsilon_0 \left(\vec{k}^{\,2} - 4\pi\hbar^2 e^2 \widetilde{\Pi}_c^0(\vec{k}, \omega) \right)} \tag{4.76}$$

Let us determine the behavior of $\Pi_c^0(\vec{q}, \omega)$,

$$\Pi_c^0(x, x') = \frac{-i}{\hbar} \text{ tr } (G_0(x, x') G_0(x', x)) \tag{4.77}$$

In momentum space it becomes

$$\widetilde{\Pi}_c^0(\vec{q}, \omega) = \frac{-2i}{\hbar} \int \frac{d^4k}{(2\pi)^4} G_0(k) G_0(q + k) \tag{4.78}$$

where $q = (\vec{q}, \omega)$, and

$$G_0(q) = \frac{1}{\omega - \frac{E(\vec{q})}{\hbar} + i \, \text{sign}(|\vec{q}| - p_F) \, \delta} \tag{4.79}$$

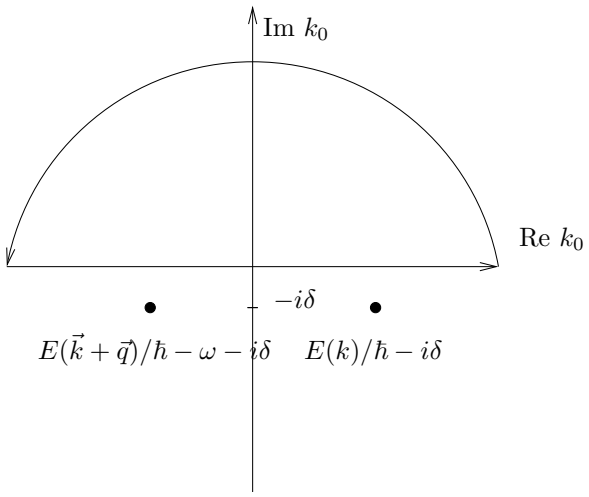

Figure 4.14: Contour used in the particle-particle channel

with $\delta = 0^+$.

We will do frequency integral first (below we have denoted by Ω the frequency)

$$\int_{-\infty}^{+\infty} \frac{d\Omega}{2\pi} \frac{1}{\left(\omega + \Omega - \frac{E(\vec{q}-\vec{k})}{\hbar} + i \text{ sign } (|\vec{q}+\vec{k}| - p_F)\, \delta\right) \left(\Omega - \frac{E(\vec{k})}{\hbar} + i \text{ sign } (|\vec{k}| - p_F)\, \delta\right)} \tag{4.80}$$

There are 4 cases:

1. $|\vec{k}+\vec{q}| > p_F$ and $|\vec{k}| > p_F$; this is the particle-particle channel. In this case the poles are located at

$$\Omega = \frac{E(\vec{k})}{\hbar} - i\delta, -\omega + \frac{E(\vec{k}+\vec{q})}{\hbar} - i\delta \tag{4.81}$$

and both are located *below* the real axis. Closing the contour on the *upper* half plane, we find that the integral vanishes (Fig.4.14).

2. $|\vec{k}+\vec{q}| < p_F$, $|\vec{k}| < p_F$. Again both singularities are on the same side of the real axis, this time **above** the real axis. Thus closing on the **lower** half plane, Fig.4.15, the integral is found to be zero. This is the hole-hole channel.

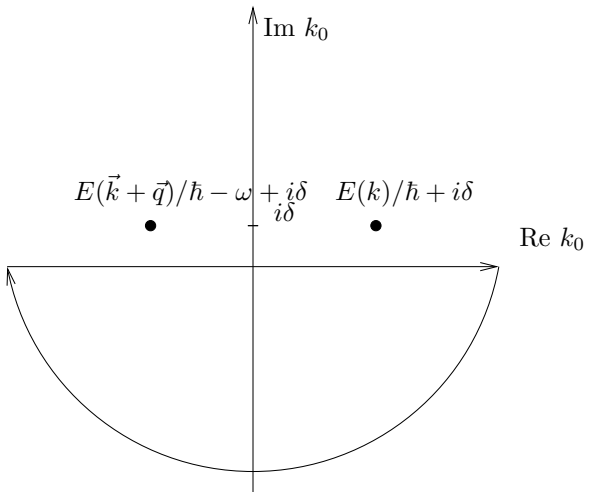

Figure 4.15: Contour used in the hole-hole channel

3. $|\vec{k}+\vec{q}| > p_F$, $|\vec{k}| < p_F$ (case (a)), and $|\vec{k}+\vec{q}| < p_F$, $|\vec{k}| > p_F$ (case (b)); this is the particle-hole channel. Now, in both cases, the two singularities lay on opposite sides of the real axis. The result of the contour integration is the same no matter where we close, but we get two contributions, one from case (a) and the other from case (b). Thus for case (a) we get the result (see Fig.4.16(a))

$$\frac{2\pi i}{2\pi}\,\theta(|k+q|-p_F)\theta(p_F-|\vec{k}|)\mathrm{Res}\left\{G_0(k+q)G_0(k),\frac{E(\vec{k})}{\hbar}+i\delta\right\} = \frac{i\theta(|\vec{k}+\vec{q}|-p_F)\theta(p_F-|\vec{k}|)}{\omega+\frac{E(\vec{k})-E(\vec{k}+\vec{q})}{\hbar}+i\delta} \tag{4.82}$$

Instead in case (b) (see Fig.4.16(b)) we get

$$-\frac{2\pi i}{2\pi}\,\theta(|k+q|-p_F)\theta(p_F-|\vec{k}|)\mathrm{Res}\left\{G_0(k+q)G_0(k),\frac{E(\vec{k})}{\hbar}-i\delta\right\} = \frac{-i\theta(p_F-|\vec{k}+\vec{q}|)\theta(|\vec{k}|-p_F)}{\omega+\frac{E(\vec{k})-E(\vec{k}+\vec{q})}{\hbar}-i\delta} \tag{4.83}$$

Therefore, we find that $\Pi_c^0(\vec{q},\omega)$ is given by the integral

$$\Pi_c^0(\vec{q},\omega) = \frac{2}{\hbar}\int \frac{d^3k}{(2\pi\hbar)^3}\left\{\frac{\theta(|\vec{k}+\vec{q}|-p_F)\theta(p_F-|\vec{k}|)}{\omega+\left(\frac{E(\vec{k})-E(\vec{k}+\vec{q})}{\hbar}\right)+i\delta} - \frac{\theta(p_F-|\vec{k}+\vec{q}|)\theta(|\vec{k}|-p_F)}{\omega+\left(\frac{E(\vec{k})-E(\vec{k}+\vec{q})}{\hbar}\right)-i\delta}\right\} \tag{4.84}$$

Upon a change in the integration variables, we get

$$\begin{aligned}\Pi_c^0(\vec{q},\omega) \;=\; & \frac{2}{\hbar}\int \frac{d^3k}{(2\pi\hbar)^3}\theta(|\vec{k}+\vec{q}|-p_F)\theta(p_F-|k|) \\ & \times\left\{\frac{1}{\omega+\left(\frac{E(k)-E(k+q)}{\hbar}\right)+i\delta} - \frac{1}{\omega-\left(\frac{E(k)-E(k+q)}{\hbar}\right)-i\delta}\right\}\end{aligned} \tag{4.85}$$

4.5.1 The Static Limit, $\omega = 0$

In the *static limit*, $\omega = 0$, the polarization operator $\Pi_c^0(\vec{q},\omega)$ becomes

$$\Pi_c^0(\vec{q},0) = -\frac{8m}{\hbar^2}\int \frac{d^3k}{(2\pi\hbar)^3}\,\frac{\theta(|\vec{k}+\vec{q}|-p_F)\theta(p_F-|\vec{k}|)}{\vec{q}^{\,2}+2\vec{k}\cdot\vec{q}} \tag{4.86}$$

For Coulomb interactions

$$\widetilde{V}(|\vec{q}|) = \frac{4\pi\hbar^2e^2}{\varepsilon_0|\vec{q}|^2} \tag{4.87}$$

we obtain the (static) dielectric function $\varepsilon(\vec{q},0)$

$$\varepsilon(\vec{q},0) = 1+\frac{4me^2}{\pi^2\varepsilon_0|\vec{q}|^2}\int_{\mathcal{R}}\frac{d^3k}{\vec{q}^{\,2}+2\vec{k}\cdot\vec{q}} = 1+\left(\frac{4}{9\pi}\right)^{1/3}r_s\frac{u(x)}{x^2} \tag{4.88}$$

where the integration is restricted to the region $\mathcal{R} = \{|\vec{k}| < p_F, |\vec{k}+\vec{q}| > p_F\}$, and x is the dimensionless variable $x = \frac{|\vec{q}|}{2p_F}$ (which measures the the momentum transfer in units of the diameter of the Fermi surface).

In Eq.(4.88) we introduced r_s, the radius of a sphere of volume $v = V/N = 1/\rho$, measured in units of the (effective) Bohr radius, which in this case is $a_0 = \hbar^2\varepsilon_0/me^2$. It is easy to see that r_s satisfies

$$p_F\frac{a_0}{\hbar}r_s = \left(\frac{9\pi}{4}\right)^{1/3} \tag{4.89}$$

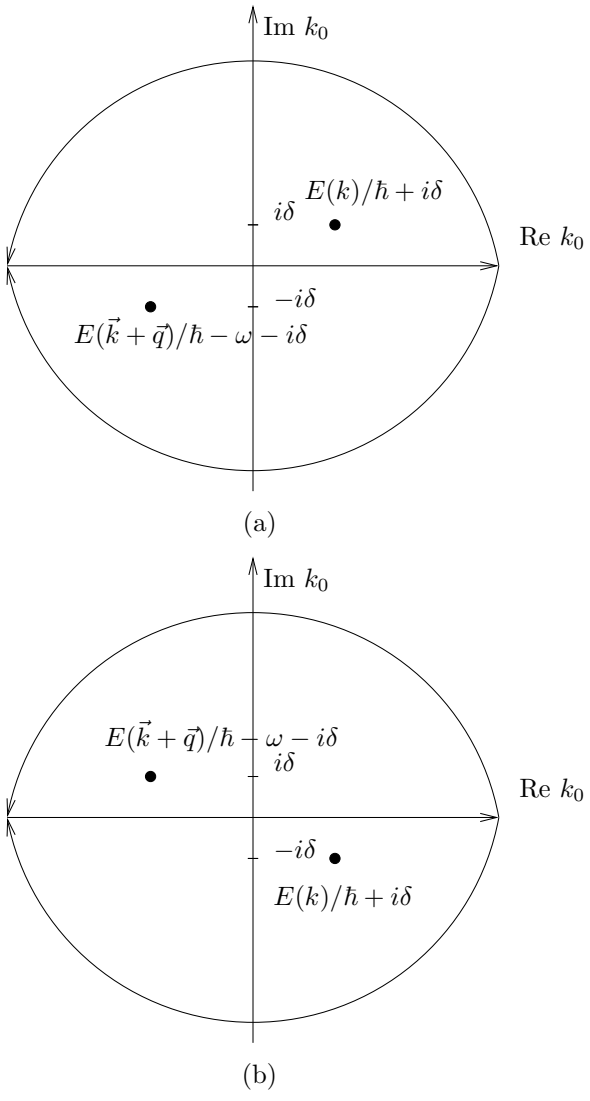

Figure 4.16: Contours used in he particle-hole channel.

or, alternatively,

$$\frac{\left(\frac{e^2}{\varepsilon_0 a_0}\right)}{E_F} = 2\left(\frac{4}{9\pi}\right)^{2/3} r_s^2 \tag{4.90}$$

Hence, r_s is a measure of the typical value of the potential energy in units of the Fermi energy. Therefore, the limit of *weak interactions* is $r_s \ll 1$, which is also achieved at (very!) high densities. In these regimes the *kinetic energy* dominates over the *potential energy*.

The dimensionless function $u(x)$ use in Eq.(4.88) is given by

$$u(x) = \frac{1}{2}\left(1 + \frac{1}{2x}(1-x^2)\log\left|\frac{1+x}{1-x}\right|\right) \tag{4.91}$$

For $q \to 0$, *i.e.* $x \to 0$, $u \to 1$ and the static dielectric function becomes

$$\varepsilon(\vec{q}, 0) \simeq 1 + \frac{\lambda^2}{|q|^2} \tag{4.92}$$

$$\lambda_{TF}^2 \equiv \frac{\hbar^2}{\xi_{TF}^2} = \frac{4}{\pi}\frac{me^2 p_F}{\varepsilon_0 \hbar^2} = \frac{4}{\pi}\left(\frac{4}{9\pi}\right)^{1/3} r_s \left(\frac{p_F}{\hbar}\right)^2 \tag{4.93}$$

where ξ_{TF} is the Thomas-Fermi *screening length*. This is the (semi-classical) *Thomas-Fermi approximation*. Within this approximation the effective static interaction potential becomes

$$\widetilde{V}_{\rm TF}(\vec{q}, 0) \simeq \frac{\left(\frac{4\pi e^2\hbar^2}{\varepsilon_0 q^2}\right)}{1 + \frac{\lambda^2}{q^2}} = \frac{4\pi\hbar^2 e^2/\varepsilon_0}{q^2 + \lambda^2} \tag{4.94}$$

which in position space is a Yukawa potential:

$$V_{\rm TF}(\vec{r}) = \int \frac{d^3q}{(2\pi\hbar)^3}\frac{4\pi e^2\hbar^2/\varepsilon_0}{q^2+\lambda^2}\, e^{i\vec{q}\cdot\vec{r}/\hbar} = \frac{e^2}{\varepsilon_0 \mid \vec{r} \mid} e^{-\frac{\mid \vec{r} \mid}{\xi_{TF}}} \tag{4.95}$$

Thus, at least in this approximation, the interactions have become short-ranged. Actually this calculation is incorrect since $u(x)$ has a weak singularity as $x \to 1$ ($\mid \vec{q} \mid \to 2p_F$). Thus, if the Fermi surface is sharp we expect extra

contributions to the dielectric function. For large $|\vec{r}|$, the correct asymptotic behavior has the power law form (Friedel, Langer and Vosko)

$$V_{\rm eff}(|\vec{r}|) \propto \frac{\cos(2p_F|\vec{r}|)}{|\vec{r}|^3} \tag{4.96}$$

instead of the (much faster) exponential decay law predicted by the Thomas-Fermi approximation. This result implies that if the Fermi surface is sharp the induced charge density caused by an external static (Coulomb) probe has the oscillatory behavior (with the power law prefactor) given above. This behavior is known as *Friedel Oscillations* and it is observed in simple metals (such as Mo) in scanning tunneling microscopy (STM) experiments.

However, we will see below that that at finite temperatures we will recover exponential screening, albeit with a temperature-dependent screening length. This is correct since at finite temperature the Fermi surface is smeared. At high temperatures the screening length approaches the classical Debye screening length.

4.5.2 Dynamic Behavior

I will not do a full analysis of $\Pi_c^0(\vec{q},\omega)$, which can be found in standard textbooks (*e.g.* Fetter and Walecka). We will discuss here its salient physical properties.

The two particle Green function in the RPA approximation has the form

$$G_c^{(2)}(q) = \frac{\widetilde{V}(q)}{1-\widetilde{V}(q)\widetilde{\Pi}_c^0(q)} \times \text{external legs} \tag{4.97}$$

As usual the poles of the Green function determine the spectrum of elementary excitations. Within this approximation, the poles are determined my the zeros of the denominator of Eq.(4.97). Hence, the spectrum of *collective excitations* (particle-hole bound states) is determined by the condition:

$$\boxed{1 = \widetilde{V}(q)\widetilde{\Pi}_c^0(q)} \tag{4.98}$$

The explicit form of this condition is

$$1 = \widetilde{V}(q) \sum_{\substack{|\vec{p}|<p_F \\ |\vec{p}+\vec{q}|>p_F}} \left\{ \frac{1}{\omega + \dfrac{E(\vec{p})-E(\vec{p}+\vec{q})}{\hbar} + i\delta} - \frac{1}{\omega - \dfrac{E(\vec{p})-E(\vec{p}+\vec{q})}{\hbar} + i\delta} \right\} \tag{4.99}$$

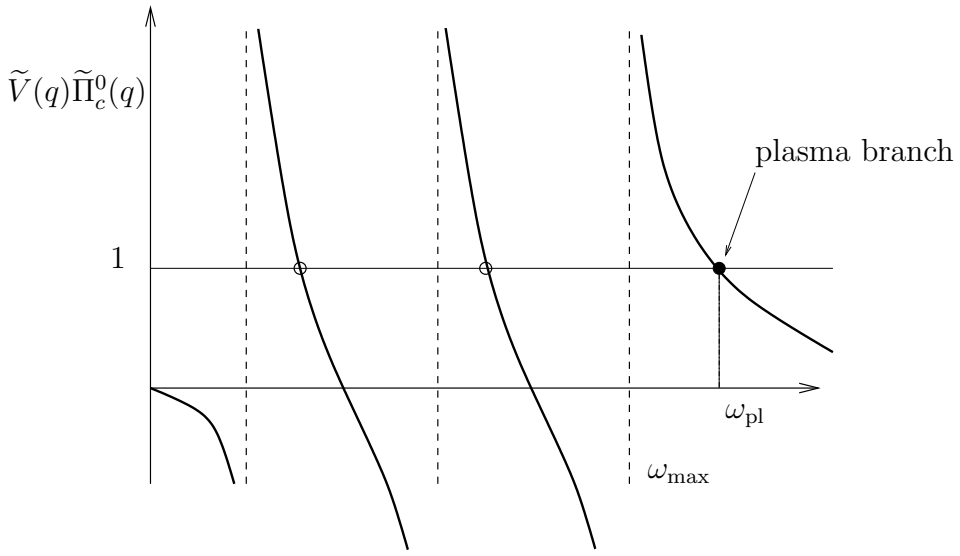

Figure 4.17: Roots of Eq.(4.99)

The roots of this equation determine the particle-hole excitations.

$\widetilde{\Pi}_c^0$ has poles at $\omega = \pm(E(\vec{p}) - E(\vec{p}+\vec{q}))/\hbar$, which is the energy of a free particle-hole pair, and the distance between two nearby poles goes to zero as the thermodynamic limit $V \to \infty$. There's a maximum frequency for such scattering states given by the largest value of $(E(\vec{p}) - E(\vec{p}+\vec{q}))/\hbar$ compatible with the restrictions $\mid \vec{p} \mid < p_F$ and $\mid \vec{p}+\vec{q} \mid > p_F$. This happens when $|\vec{p}| = p_F$ and $\vec{p}$ is parallel to $\vec{q}$. This implies that $\hbar\omega_{\rm max} = \frac{p_F|\vec{q}|}{m} + \frac{\vec{q}^{\,2}}{2m}$. Thus the continuum of particle-hole states has the range $0 \le \omega \le \omega_{\rm max}$ and it shrinks to zero as $\vec{q} \to 0$.

The extra root at $\omega = \omega_{\rm pl}$, known as the *plasma frequency*, represents a *collective excitation* which survives as $\vec{q} \to 0$. This root lies outside the particle-hole continuum and hence it represents a stable particle-hole bound state. Thus in this frequency regime the polarization operator$\widetilde{\Pi}_c^0(\vec{q},\omega)$ is purely real. By keeping the small $\vec{q}$ behavior only we can approximate

$$\widetilde{\Pi}_c^0(q) = \sum_{|\vec{p}|<p_F} \frac{\vec{q}^{\,2}}{m\omega^2} + O(q^4) = \frac{\vec{q}^{\,2}\rho}{m\omega^2} + O(q^4) \qquad (4.100)$$

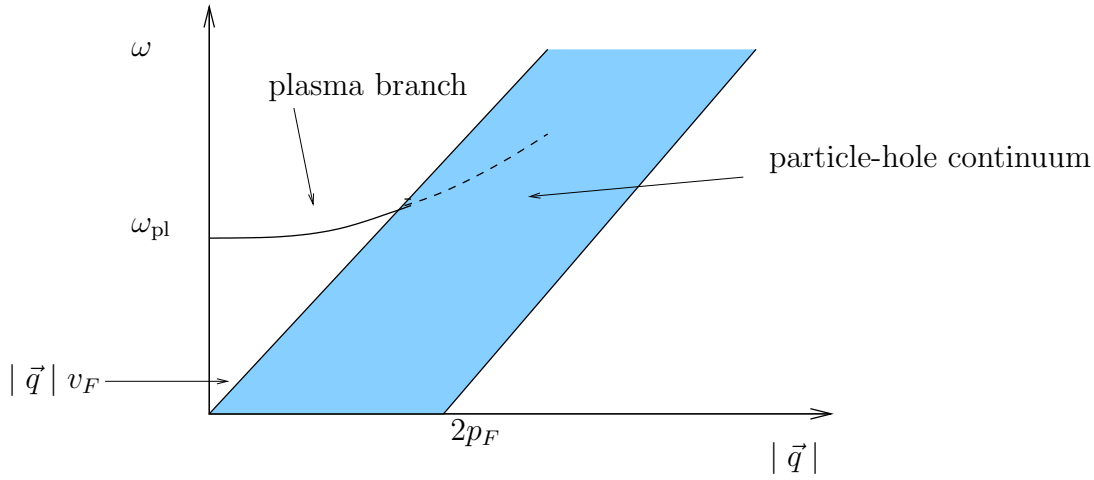

Figure 4.18: Particle-hole plasma bound state and continuum spectrum of unbound particle-hole pairs.

In this limit the dynamic dielectric function becomes

$$\varepsilon(\vec{q},\omega) = 1 - \frac{4\pi e^2}{\varepsilon_0 \vec{q}^{\,2}} \frac{\rho \vec{q}^{\,2}}{m\omega^2} = 1 - \frac{\omega_{\rm pl}^2}{\omega^2} \tag{4.101}$$

where

$$\omega_{\rm pl} = \sqrt{\frac{4\pi e^2 \rho}{\varepsilon_0 m}} \tag{4.102}$$

is the plasma frequency. Notice the important cancellation between the pole in $\vec{q}^{\,2}$ in the Coulomb potential $\widetilde{V}(\vec{q})$ and the $\vec{q}^{\,2}$ dependence of the polarization operator leading to a finite plasma frequency. Thus, the collective mode is *gapped*. In contrast, if the interactions had been short ranged to begin with, the $\vec{q}^{\,2}$ dependence of $\widetilde{\Pi}_c^0(\vec{q},\omega)$ would have implied the existence of a collective mode with a *linear* dispersion $\omega(\vec{q}) \propto |\vec{q}|$. This is what happens in *neutral* Fermi systems such as in the normal phase of liquid ^{3}He, where this collective mode is known a *zero sound*.

In summary, the spectrum of the two-particle Green function consists of a particle-hole collective mode (the plasma branch) and a particle-hole continuum.